



Pervaporation properties and a semi-empirical model for removal of VOCs from water using a propyl functionalized silica membrane

Sadao Araki*, Daisuke Gondo, Hideki Yamamoto

Department of Chemical, Energy and Environmental Engineering, Kansai University, 3-35 Yamatecho 3-chome, Suita-shi, Osaka 564-8680, Japan, email: araki_sa@kansai-u.ac.jp (S. Araki)

Received 11 April 2018; Accepted 3 September 2018

ABSTRACT

A propyl-functionalized silica membrane (PrFS membrane) was prepared to remove volatile organic compounds such as ethyl acetate (EA), methyl ethyl ketone from aqueous solutions by pervaporation. The effects of feed organic concentration (3–7 wt%) and temperature (295–325 K) on the flux and separation factor were confirmed. Based on these results, the simple calculation equation was developed by using the organic concentration, temperature and Hansen solubility parameters. The flux values calculated using this equation showed excellent agreement with the measured fluxes with coefficient of determination (R^2) of 0.92.

Keywords: Pervaporation; Hydrophobic membrane; Propyltrimethoxysilane; Silica

1. Introduction

Pervaporation is an important technique that involves the use of membranes to separate and recover volatile organic compounds from liquid mixtures as vapors. Ceramics, polymers, metal organic frameworks and these composites were reported as membrane materials for pervaporation [1–8]. Inorganic membranes are generally inferior to polymeric membranes in terms of formability and cost. However, inorganic membranes have received considerable interest in terms of their application to pervaporation because of their high chemical and heat-resistance properties. Further development of inorganic membrane is required to reduce the energy consumption and membrane area. It is necessary to perceive the key factor that affects the permeance for the development of the performance of membrane.

Pervaporation transport through the pores of an inorganic membrane is usually described in terms of an adsorption-diffusion mechanism based on the solution-diffusion model for polymeric membranes [9,10]. According to this mechanism, permeate materials in the

liquid-phase on the feed side would be adsorbed on the pores of the inorganic membrane. These materials would diffuse through the membrane, and then be desorbed into the vapor phase on the permeate side due to the concentration gradient. Therefore, the key factors of pervaporation transport include the affinity between permeate materials and membrane materials, pore structure of the membrane and the physicochemical properties of permeate materials. Although there are many reports concerning transport mechanisms of organic and inorganic membranes, mostly the mechanisms are used for explanations of the permeation results.

As a predictive model, Mujiburohman et al. [11] reported the empirical formula based on dimensionless numbers that they used as a predictive model to estimate the flux of pervaporation using polymeric membranes. Bowen et al. [10] reported that the correlations observed between the separation factors and the feed fugacities could be used to predict pervaporation. However, some experiments of pervaporation are required to accurately define the relationships between the separation factors and the feed fugacities. In other words, it is difficult to predict the most suitable membrane materials for the separation of certain substances.

* Corresponding author.

In a previous study, we prepared hydrophobic silica membranes with methyl, propyl, iso-butyl, *n*-hexyl or phenyl groups, respectively, to separate and recover volatile organic compounds (VOCs) such as ethyl acetate (EA), methyl ethyl ketone (MEK), acetone and 1-butanol (1-BtOH) from aqueous solutions [12]. These membranes have similar average pore size and membrane thickness regardless of the difference in their functional groups. Therefore, diffusivities of the organic compounds through the membranes were considered to be the same. In other words, the permeance was dictated by the affinities of the organic compounds for the membrane material. We used the Hansen solubility parameter (HSP) to estimate the affinity between the organic compounds and the membrane materials. HSP values are based on the three cohesive energies per unit molar volume and can be used to estimate the compatibility and the dispersibility [13–17]. The HSP consists of several components, including the dispersion force (δ_d [MPa^{1/2}]), the dipole interaction force factor (δ_p [MPa^{1/2}]) and the hydrogen-bonding force factor (δ_h [MPa^{1/2}]). The compatibility between substance A and B can be generally estimated by R_a , which is the distance between the HSPs of two substances in a three-dimensional HSP diagram.

$$R_a = [4(\delta_{dA} - \delta_{dB})^2 + (\delta_{pA} - \delta_{pB})^2 + (\delta_{hA} - \delta_{hB})^2]^{1/2} \quad (1)$$

We found that there was a linear relationship between the logarithms of the fluxes and the R_a values regardless of the membrane materials and the organic compounds.

$$J_{\text{organic}} = a \times M \times e^{(b \times R_a)} \quad (2)$$

where J_{organic} is the flux of the organic compound (kg m⁻² h⁻¹), M is the molecular weight (g mol⁻¹), and a (kmol m⁻² h⁻¹) and b (MPa^{-1/2}) are constants. This semi-empirical equation based on the HSP could be used to identify suitable membrane materials and estimate the permeation flux of certain organic compounds. On the other hand, this equation is limited at 5 wt% in the feed solution at 295 K. In other words, the dependent properties of feed concentration and temperature on this equation are not clear. Therefore, we measured pervaporation properties of a hydrophobic silica membrane with propyl groups, which showed high organic fluxes and separation factors [12], for EA, MEK, acetone, 1-BtOH, tetrahydrofuran (THF) and methyl acetate (MA) at feed concentrations ranging from 1 to 7 wt% and the temperatures ranging from 295 to 325 K.

2. Materials and methods

2.1. Membrane preparation

A propyl functionalized silica membrane (PrFS membrane) was prepared on an alumina support with the γ -alumina layer by a sol-gel method using *n*-propyltrimethoxysilane (PrTMS) [12]. The α -alumina supports (outer diameter: 10 mm, inner diameter: 6 mm, length: 35 mm) had an average pore size 0.15 μ m with average porosity: 40%. Cetyl-trimethylammonium bromide (0.008 mol), PrTMS (0.1 mol) and 7.5 mL of 1 mol L⁻¹ HNO₃ were added in 25 mL of ethanol, and then the mixture was stirred at room temperature for 3 h. The alumina support

was immersed in the sol for 60 s and then calcined at 453 K after drying at room temperature. The PrFS membrane was characterized by the permeometry and field emission scanning electron microscopy (FE-SEM).

2.2. Pervaporation

The pervaporation properties of the PrFS membrane were measured by using a home-made pervaporation apparatus. EA, MEK, acetone, 1-BtOH, THF and MA were used as the organic compounds, each at the organic concentration from 1 wt% to 7 wt% in feed solution. The PrFS membrane was immersed in the aqueous solution at temperature ranging from 295 to 325 K. Pressure of inner side of membrane decreased to about 3 Pa by a vacuum pump. Permeated gas was condensed to recover for 1 h by liquid nitrogen. The flux (J) and separation factor of the organic compound to water (α) were calculated by the following equations, respectively, based on the mass and composition of the permeate measured using a Karl Fischer water meter (AQV-2100, Hiranuma Industry, Japan). When the permeated mixture is separated to two phases, a certain amount of ethanol was added to form a homogenous solution. Standard deviations of feed and permeate concentrations are 0.44 and 0.34 wt%, respectively.

$$J = W/At \quad (3)$$

$$\alpha = \frac{\frac{y_{\text{organic}}}{x_{\text{organic}}}}{\frac{y_{\text{water}}}{x_{\text{water}}}} \quad (4)$$

where J is the flux (kg m⁻² h⁻¹), W is the permeate mass (kg), A is the membrane area (m²), t is the measurement time (h), and x and y are the amount of substance or mass fractions of water and organic compound in the feed (x) and permeate (y).

2.3. Correction of the HSPs to the temperature

The HSP values of the organic compounds were corrected for temperature because the HSP values at 25°C are listed in the literature [13]. The following equations were used to correct the HSP values for temperature [18].

$$\delta_d = \left(\frac{V_{298}}{V}\right)^{1.25} \delta_{d298} \quad (5)$$

$$\delta_p = \left(\frac{V_{298}}{V}\right)^{0.5} \delta_{p298} \quad (6)$$

$$\delta_h = \delta_{h298} \cdot \exp \left[1.32 \times 10^{-3} (298 - T) + \ln \left(\frac{V_{25^\circ\text{C}}}{V} \right)^{0.5} \right] \quad (7)$$

where V is the molar volume, T is the temperature (K) and a subscript of 298 indicates a value determined at 298 K. The densities of the different organic compounds at each

temperature were measured to obtain the molar volume by using density meter (DMA4500, Anton Paar, Austria). The HSP of the PrFS membrane was not corrected based on the assumption that any changes in the volume of the PrFS membrane would be negligible.

3. Results and discussion

3.1. Characterization of PrFS membrane

The result of permoporometry using ethyl acetate as condensed gas for the PrFS membrane is shown in Fig. 1. The average pore diameter was about 1.1 nm. Although the pores with diameters >2 nm were observed, the pores with diameters <2 nm was made up of a majority of the PrFS membrane. This pore structure was similar with that of previous work [12]. Cross-sectional FE-SEM image is shown in Fig. 2. Three layers of PrFS, γ -alumina and α -alumina support was clearly observed and show excellent adhesion and no detectable pinholes or cracks. The thickness of the PrFS layer was about 1 μm which is also in a good agreement with the previous work [12].

3.2. Pervaporation

The effects of feed organic concentration (3–7 wt%) and temperature (295–325 K) on the flux and the separation factor were confirmed for the organic aqueous solutions of EA, acetone, 1-BtOH, MEK, THF and MA. The effects of concentration of organic compounds in aqueous solution on fluxes of water and organic compounds, as well as the separation factors of these mixtures at 295 K through the PrFS membrane are shown in Fig. 3. As shown in Fig. 3(a), the EA flux increased considerably from 0.2 to 0.9 $\text{kg m}^{-2} \text{h}^{-1}$ for the EA/water system at EA concentration ranging from 1 to 7 wt%. The other systems also showed the increase of organic fluxes with the concentrations. This will be due to the increase of driving force with concentration of organic compounds in feed solutions. On the other hand, water fluxes were almost the same value of about 0.15 $\text{kg m}^{-2} \text{h}^{-1}$

regardless of organic compounds and concentration in feed. In addition, the water flux for the pervaporation of pure water through the PrFS membrane was 0.17 $\text{kg m}^{-2} \text{h}^{-1}$, which is almost identical to those of the organic compound mixtures. Bowen et al. [10] reported that the water flux for the pervaporation of aqueous mixtures of organic compounds through a Ge-ZSM5 membrane decreased significantly as the kinetic diameter of the organic compounds increased. This result was suggested that the adsorbed organic compounds could inhibit the water permeation through the zeolite pores. The differences observed in the of water fluxes through the PrFS membrane and zeolite membranes could, therefore, be attributed to the differences in the pore structures of these materials. The pore structure of zeolite is rigid, and the pore size is uniform. On the other hand, the PrFS membrane has amorphous structure and a broad pore distribution. In addition, Si-O-based rings have a pore size around 0.3 nm [19]. With this in mind, we concluded that the water molecules were permeating through the Si-O-based rings of the amorphous silica network instead of permeating through pores with propyl groups that would allow for the permeation of the organic compounds.

The effects of temperature on the fluxes of the organic compounds and water, as well as the separation factors were confirmed using aqueous mixtures containing 5 wt% of the different organic compound (Fig. 4). Both the organic compounds and the water fluxes increased with temperature, and the separation factors for all systems slightly decreased with the temperature. Especially, the EA flux showed the high value of about 2.2 $\text{kg m}^{-2} \text{h}^{-1}$ at 325 K. These results were due to the increases of driving force and diffusibility through the membrane with increasing feed temperature regardless of the type of permeated materials [20]. In addition, the water fluxes at each temperature showed similar values regardless of organic compounds.

3.3. Modeling of fluxes

The relationships between the logarithms of the organic fluxes and the R_a values at 295 K are shown in Fig. 7. The coefficient of determination R^2 was greater than 0.94 for all feed of the concentrations ranging from 1 to 7 wt%. This result, therefore, indicated that the logarithms of the organic fluxes were strongly correlated with the R_a values for the

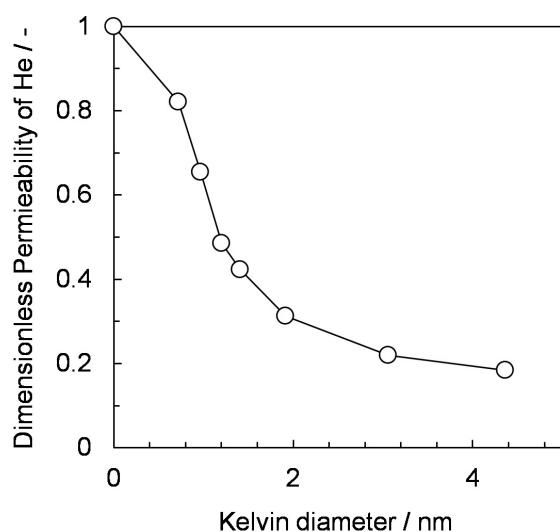


Fig. 1. Dimensionless permeability of He as a function of the Kelvin diameter for PrFS membrane.

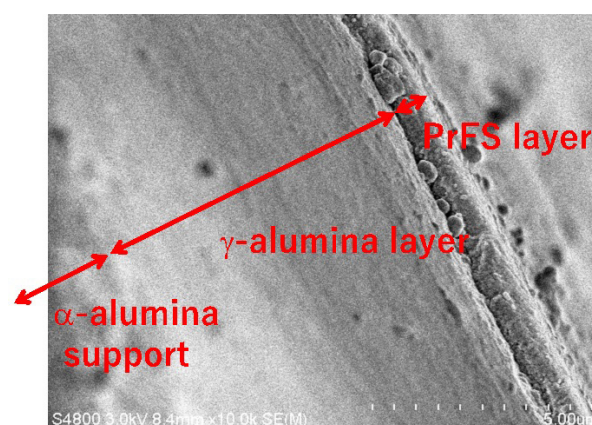


Fig. 2. FE-SEM image of cross-section of PrFS membrane.

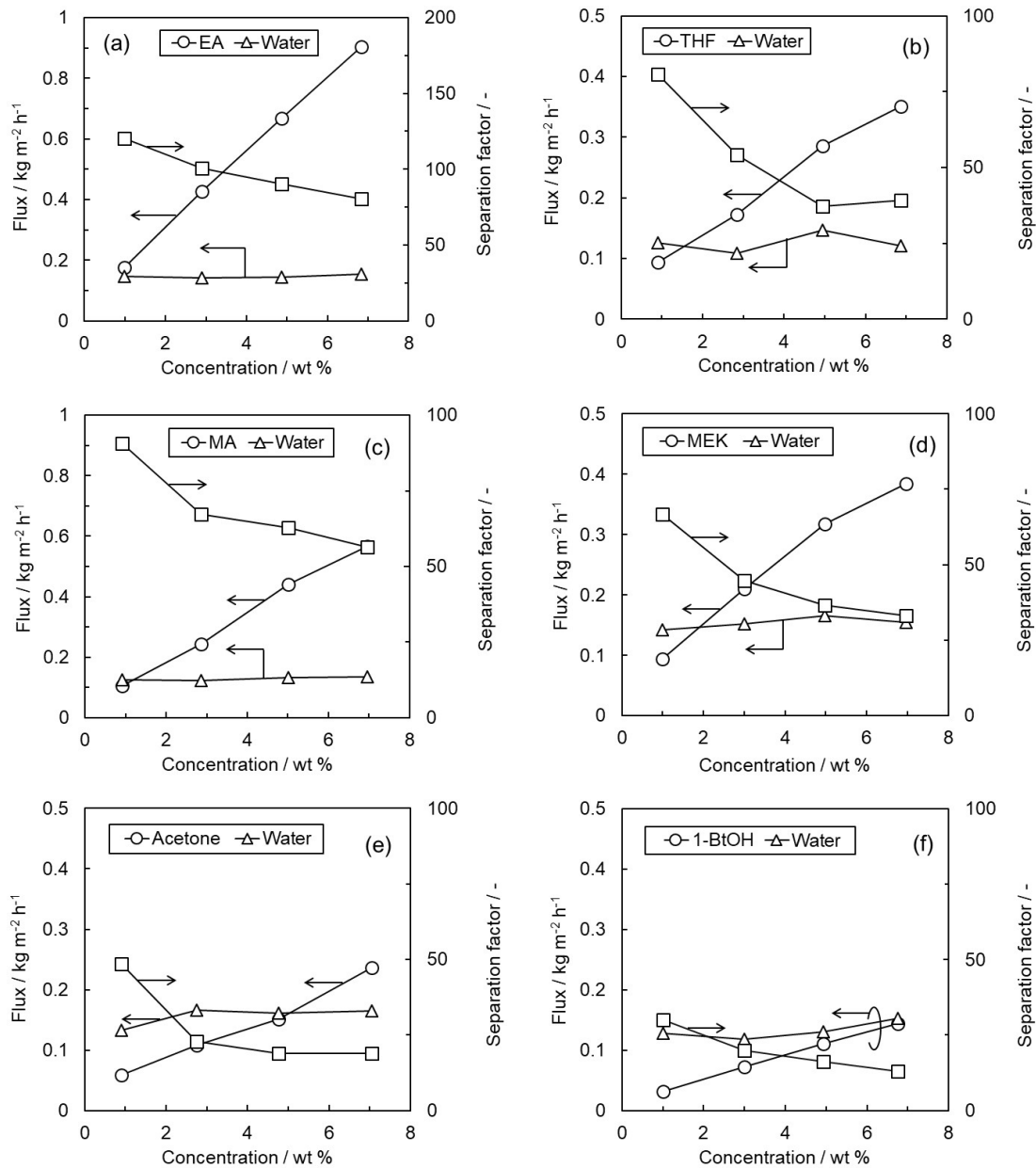


Fig. 3. Relationship between the organic feed concentration and the pervaporation properties for the organic compounds/water solutions of (a) EA, (b) THF, (c) MA, (d) MEK, (e) acetone and (f) 1-BtOH at 295 K.

feed concentration ranging from 1 to 7 wt%. Interestingly the b value in Eq. (2) was about $-0.2 \text{ MPa}^{-1/2}$ regardless of feed concentration, whereas the a value showed a linear relationship with the feed concentration. These results suggested that the concentration could be expressed as the driving force.

Fig. 5(b) shows the relationship between the R_a values and the logarithms of the organic fluxes at each temperature for 5 wt% of organic compounds in water. Although the R^2 values decreased compared with those of Fig. 5(a), the logarithms of the organic fluxes correlated with R_a with R^2 values greater than 0.86. Generally, the adsorption decreased with increasing temperature. However, this result suggested that the affinity between the membrane and the organic compounds was

considerably affected by the organic flux at temperature up to 325 K. The b value was about $-0.2 \text{ MPa}^{-1/2}$ regardless of the temperature. Amazingly, there was no large dependency between the b value and concentration and temperature.

Based on these results, Eq. (2) was developed to the following equation.

$$J_{\text{organic}} = 7.11 \times 10^3 M \cdot x \cdot e^{\frac{-0.205RTRa - 24.7 \times 10^3}{RT}} \quad (8)$$

where J_{organic} is the organic flux ($\text{kg m}^{-2} \text{ h}^{-1}$), T is the temperature (K), M is the molecular weight (g mol^{-1}), R is the molar gas constant ($\text{J K}^{-1} \text{ mol}^{-1}$) and x is the organic mass fraction.

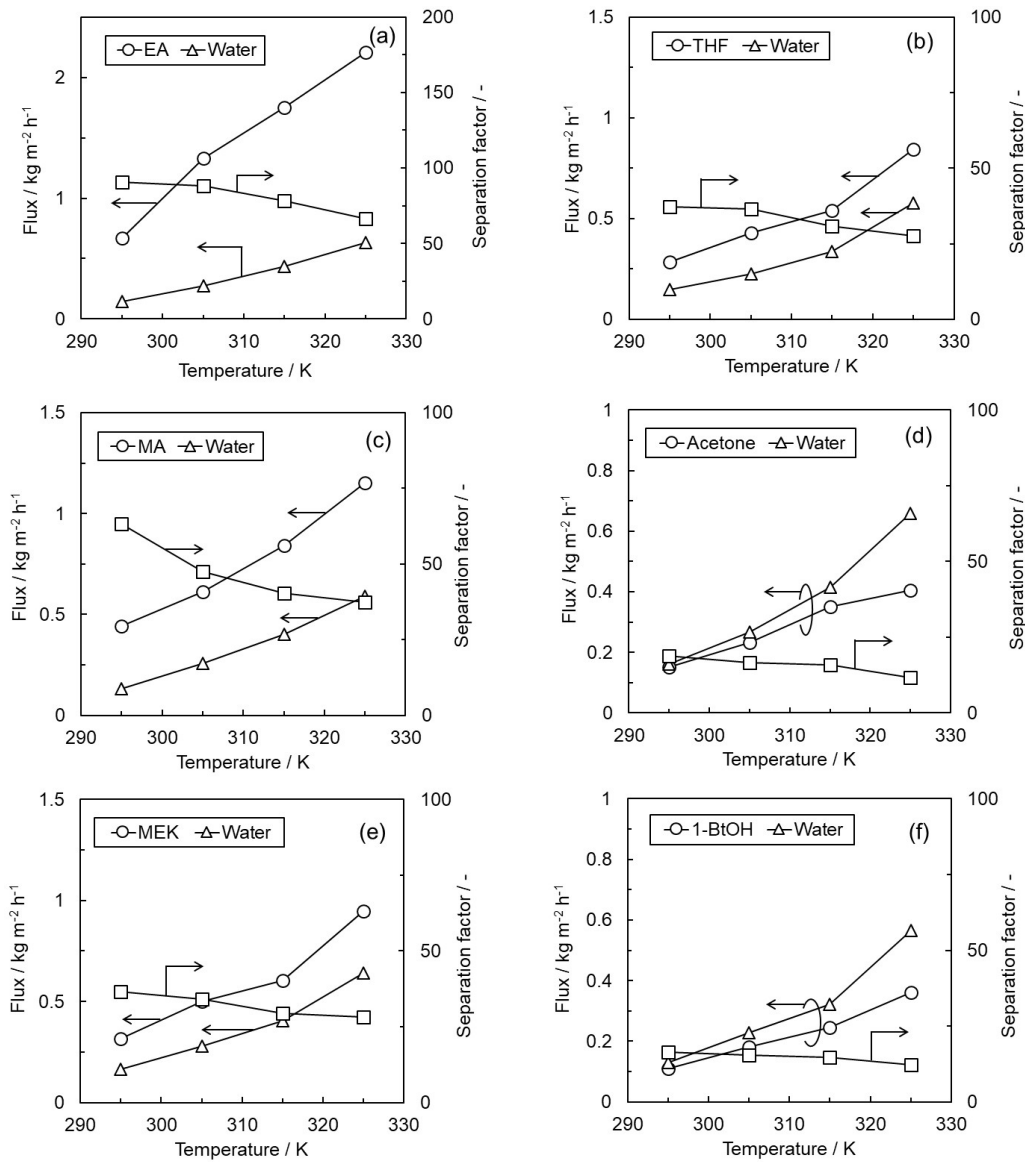


Fig. 4. Relationship between the temperature and the pervaporation properties for the organic compound (5 wt%)/water solutions of (a) EA, (b) THF, (c) MA, (d) MEK, (e) acetone, and (f) 1-BtOH.

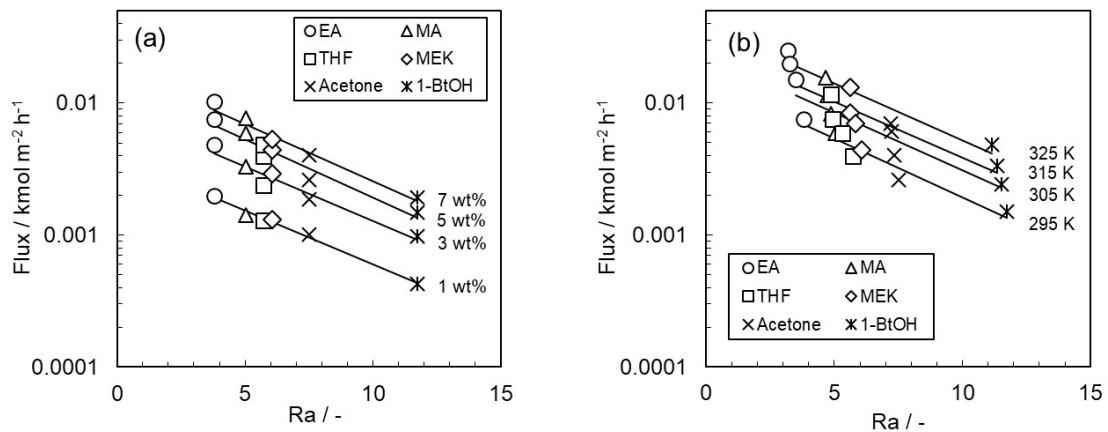


Fig. 5. Effects of (a) the organic concentration and (b) the temperature on the relationship between R_a and logarithms of flux.

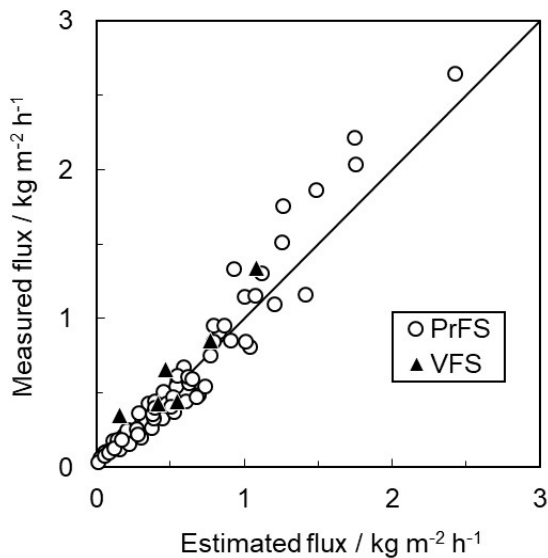


Fig. 6. Relationship between the estimated and the measured fluxes.

This equation form is similar with the following equation based on the adsorption–diffusion model in the case of gas permeation through a microporous membrane at a certain pressure difference [21].

$$J_g = J_0 e^{\frac{\Delta H_a - \Delta E}{RT}} \quad (9)$$

where J_g is the gas flux ($\text{kg m}^{-2} \text{h}^{-1}$), J_0 is the pre-exponential factor ($\text{kg m}^{-2} \text{h}^{-1}$), ΔH_a is the adsorption heat (J mol^{-1}) and ΔE is the activation energy (J mol^{-1}). Therefore, the value of 24.7 kJ mol^{-1} corresponds to the activation energy and $-0.205 RT_{R_a}$ is likely to correspond to the adsorption heat.

Fig. 6 shows the relationship between the organic flux values for organic concentration ranging from 1 to 7 wt% at temperature ranging from 295 to 325 K and the calculated flux values, which were determined by Eq. (8). The R^2 value between the measured and the calculated flux values was 0.92, thereby confirming that our equation can be used accurately to calculate the flux values of different organic compounds over a wide range of organic concentrations and temperatures.

As described previously, the water flux depended on the feed temperature and did not depend on the type of the organic compounds and concentrations. The relationship between logarithms of the water flux and the reciprocal of temperature is shown in Fig. 7. The least squares method to correlate water flux is as shown in Eq. (10). This equation was used for water concentrations ranging from 93 wt% to 100 wt% because no relationship between the water flux and the water concentration was observed, as shown in Fig. 3.

$$J_{\text{water}} = 5.36 \times 10^5 e^{-37.0 \times 10^3 / RT} \quad (10)$$

where J_{water} is the water flux ($\text{kg m}^{-2} \text{h}^{-1}$) and T is the temperature (K). This equation showed a strong correlation with the measured fluxes with R^2 values of 0.97.

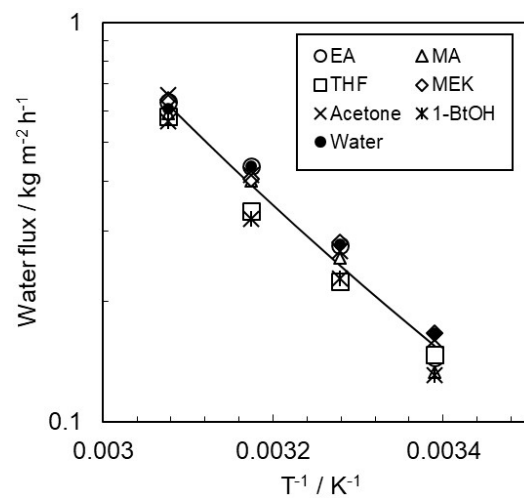


Fig. 7. Relationship between the temperature and the water flux for the pervaporation of the organic compound (5 wt%)/water solutions.

On the other hand, we have already known that Eq. (2) can estimate the organic flux regardless of the functional groups of the hydrophobic silica membranes if the same membrane preparation procedure and the same porous support were used [12]. The relationship between calculated fluxes and measured fluxes for the vinyl-functionalized silica membrane are also shown in Fig. 6 [22]. These relationships lied within the range of variation. Therefore, these equations can be used to estimate the organic flux and separation factor values of organic compounds for organic concentrations ranging from 1 to 7 wt% at temperatures ranging from 295 to 325 K without conducting any experiments for the pervaporation using the hydrophobic silica membranes to separate organic compounds from aqueous solutions.

4. Conclusions

In this study, we have determined the fluxes and separation factors of aqueous solutions containing 1–7 wt% of EA, MEK, acetone, 1-BtOH, THF and MA for the pervaporation through the PrFS membrane at temperature in the range of 295–325 K. All of the organic fluxes increased with increasing the organic concentration and temperature. In contrast, the water flux was independent of the type of organic compounds and concentration although the water flux increased with increasing temperature.

The relationship between the logarithms of the organic fluxes and the R_a values moved in parallel according to the organic concentration and the temperature. In other words, the gradient of each slope was similar regardless of the organic concentration or the temperature, whereas the intercept changed depending on both of these factors. A correlation equation based on these results showed good agreement with the measured values with a correlation coefficient of 0.92. This equation could, therefore, be used to estimate the organic flux of different organic compounds for certain concentration and temperature values for the pervaporation using the hydrophobic silica membranes to separate organic compounds from aqueous solutions.

Acknowledgment

This work was partially supported by MEXT-Supported Program for the Strategic Research Foundation at Private Universities, 2012–2016.

References

- [1] Q. Wang, Y. Lu, N. Li, Preparation, characterization and performance of sulfonated poly(styrene-ethylene/butylene-styrene) block copolymer membranes for water desalination by pervaporation, *Desalination*, 390 (2016) 33–46.
- [2] Y. Li, J. Shen, K. Guan, G. Liu, H. Zhou, W. Jin, PEBA/ceramic hollow fiber composite membrane for high-efficiency recovery of bio-butanol via pervaporation, *J. Membr. Sci.*, 510 (2016) 338–347.
- [3] C. Ding, X. Zhang, C. Li, X. Hao, Y. Wang, G. Guan, ZIF-8 incorporated polyether block amide membrane for phenol permselective pervaporation with high efficiency, *Sep. Purif. Technol.*, 166 (2016) 252–261.
- [4] X. Dong, Y.S. Lin, Synthesis of an organophilic ZIF-71 membrane for pervaporation solvent separation, *Chem. Commun.*, 49 (2013) 1196–1198.
- [5] X.M. Wu, Q.G. Zhang, F. Soyekwo, Q.L. Liu, A.M. Zhu, Pervaporation removal of volatile organic compounds from aqueous solutions using the highly permeable PIM-1 membrane, *AIChE J.*, 62 (2016) 842–851.
- [6] B. Elyassi, M.Y. Jeon, M. Tsapatsis, K. Naraashimharao, S.N. Basahel, S. Al-Thabaiti, Ethanol/water mixture pervaporation performance of b-oriented silicalite-1 membranes made by gel-free secondary growth, *AIChE J.*, 62 (2016) 556–563.
- [7] J. Liu, J. Chen, X. Zhan, M. Fang, T. Wang, J. Li, Preparation and characterization of ZSM-5/PDMS hybrid pervaporation membranes: laboratory results and pilot-scale performance, *Sep. Purif. Technol.*, 150 (2015) 257–267.
- [8] N. Kosinov, C. Auffret, G.J. Borghuis, V.G.P. Sripathi, E.J.M. Hensen, Influence of the Si/Al ratio on the separation properties of SSZ-13 zeolite membranes, *J. Membr. Sci.*, 484 (2015) 140–145.
- [9] D. Shah, K. Kissick, A. Ghorpade, R. Hannah, D. Bhattacharyya, Pervaporation of alcohol–water and dimethylformamide–water mixtures using hydrophilic zeolite NaA membranes: mechanisms and experimental results, *J. Membr. Sci.*, 179 (2000) 185–205.
- [10] T.C. Bowen, S. Li, R.D. Noble, J.L. Falconer, Driving force for pervaporation through zeolite membranes, *J. Membr. Sci.*, 225 (2003) 165–176.
- [11] M. Mujiburohman, K.A. Mahdi, A. Elkamel, Predictive model of pervaporation performance based on physicochemical properties of permeant-membrane material and process conditions, *J. Membr. Sci.*, 381 (2011) 1–9.
- [12] S. Araki, D. Gondo, S. Imasaka, H. Yamamoto, Permeation properties of organic compounds from aqueous solutions through hydrophobic silica membranes with different functional groups by pervaporation, *J. Membr. Sci.*, 514 (2016) 458–466.
- [13] C.M. Hansen, Hansen Solubility Parameters – A User’s Handbook, CRC Press, Boca Raton, FL, 2007.
- [14] H. Launay, C.M. Hansen, K. Almdal, Hansen solubility parameters for a carbon fiber/epoxy composite, *Carbon*, 45 (2007) 2859–2865.
- [15] J.B. Petersen, J. Meruga, J.S. Randle, W.M. Cross, J.J. Kellar, Hansen Solubility Parameters of Surfactant-Capped Silver Nanoparticles for Ink and Printing Technologies, *Langmuir*, 30 (2014) 15514–15519.
- [16] M. Morimoto, T. Sato, S. Araki, R. Tanaka, h. Yamamoto, S. Sato, T. Takanohashi, Mapping the Degree of Asphaltene Aggregation, Determined Using Rayleigh Scattering Measurements and Hansen Solubility Parameters, *Energy Fuels*, 29 (2015) 2808–2812.
- [17] T. Sato, Y. Hamada, M. Sumikawa, S. Araki, H. Yamamoto, Solubility of Oxygen in Organic Solvents and Calculation of the Hansen Solubility Parameters of Oxygen, *Ind. Eng. Chem. Res.*, 53 (2014) 19331–19337.
- [18] L.L. Williams, J.B. Rubin, H.W. Edwards, Calculation of Hansen Solubility Parameter Values for a Range of Pressure and Temperature Conditions, Including the Supercritical Fluid Region, *Ind. Eng. Chem. Res.*, 43 (2004) 4967–4972.
- [19] S.T. Oyama, D. Lee, P. Hacarlioglu, R.F. Saraf, Theory of hydrogen permeability in nonporous membranes, *J. Membr. Sci.*, 224 (2004) 45–53.
- [20] P. Shao, R.Y.M. Huang, Polymeric membrane pervaporation, *J. Membr. Sci.*, 287 (2007) 162–179.
- [21] D. Lee, S.T. Oyama, Gas permeation characteristics of a hydrogen selective supported silica membrane, *J. Membr. Sci.*, 210 (2002) 291–306.
- [22] S. Araki, A. Okabe, A. Ogawa, D. Gondo, S. Imasaka, Y. Hasegawa, K. Sato, K. Li, H. Yamamoto, Preparation and pervaporation performance of vinyl-functionalized silica membranes, *J. Membr. Sci.*, 548 (2018) 66–72.